



Research article

Potential drug-like inhibitors of Group 1 influenza neuraminidase identified through computer-aided drug design

Jacob D. Durrant^{a,*}, J. Andrew McCammon^{b,c,d}

^a Biomedical Sciences Program, University of California San Diego, 9500 Gilman Drive, La Jolla, CA 92093-0365, United States

^b Department of Chemistry & Biochemistry, NSF Center for Theoretical Biological Physics, National Biomedical Computation Resource, University of California San Diego, La Jolla, CA 92093, United States

^c Department of Pharmacology, University of California San Diego, La Jolla, CA 92093, United States

^d Howard Hughes Medical Institute, University of California San Diego, La Jolla, CA 92093, United States

ARTICLE INFO

Article history:

Received 1 October 2009

Received in revised form 15 January 2010

Accepted 26 March 2010

Keywords:

Influenza

Neuraminidase

Drug design

Oseltamivir

Flu

H1N1

ABSTRACT

Pandemic (H1N1) influenza poses an imminent threat. Nations have stockpiled inhibitors of the influenza protein neuraminidase in hopes of protecting their citizens, but drug-resistant strains have already emerged, and novel therapeutics are urgently needed. In the current work, the computer program AutoGrow is used to generate novel predicted neuraminidase inhibitors. Given the great flexibility of the neuraminidase active site, protein dynamics are also incorporated into the computer-aided drug-design process. Several potential inhibitors are identified that are predicted to bind to neuraminidase better than currently approved drugs.

© 2010 Elsevier Ltd. All rights reserved.

1. Introduction

Influenza is caused by RNA viruses of the family Orthomyxoviridae. While not generally life threatening in healthy adults, the virus occasionally mutates into more deadly forms and has been responsible for several pandemics in the last century. Recently, a new strain of pandemic influenza (H1N1) capable of infecting humans has been identified (Dawood et al., 2009), with a U.S. hospitalization rate of about 9%. Additionally, a distinct strain of avian influenza (H5N1) arose in 1997 that may cause a similar global pandemic in the future (Abdel-Ghafar et al., 2008).

In preparation for pandemic influenza, many nations have stockpiled inhibitors of the influenza protein neuraminidase (Oxford et al., 2004). Following formation, influenza viral particles remain bound to cell membranes via sialic-acid residues. Neuraminidase cleaves these residues, releasing the virus and enabling viral propagation (De Clercq and Neyts, 2007). Neuraminidase is the target of several FDA-approved drugs, including zanamivir and oseltamivir (Oxford et al., 2004), because it is essential for viral propagation and has a well-conserved active site (Kobasa et al., 1999). Unfortunately, drug-resistant strains have recently emerged (Kiso et al.,

2004; Beigel et al., 2005; de Jong et al., 2005; De Clercq, 2006), and the need for novel inhibitors is great.

Motivated by the urgent need for new influenza therapeutics, we used AutoGrow (Durrant et al., 2009), a recently developed computer-aided drug-design program, to guide the design of several potential neuraminidase inhibitors predicted to bind better than currently approved drugs.

2. Material and methods

2.1. Accounting for protein flexibility

To account for protein flexibility, we drew upon a molecular dynamics simulation of neuraminidase that has been described previously (Cheng et al., 2008). Protein conformations extracted from this 40-ns simulation were clustered into 27 groups by root-mean-square-deviation (RMSD) conformational clustering using the *gromos* clustering algorithm, as implemented in the GRO-MOS++ analysis software (Daura et al., 1999; Christen et al., 2005). In brief, an RMSD distance was calculated for each pair of protein conformations extracted from the MD simulation. Those pairs with associated RMSD distances greater than 1.3 Å were discarded. The single conformation most frequently present in the remaining pairs, together with the other corresponding conformation of each pair, were merged into a list of conformations called the first cluster.

* Corresponding author. Tel.: +1 858 822 0169; fax: +1 858 534 4974.

E-mail address: jdurrant@ucsd.edu (J.D. Durrant).

The conformations of the first cluster were subsequently removed from the pool of conformations extracted from the MD simulation, and the process was repeated until no conformations remained. The centroid of each cluster was selected, producing an ensemble of 27 unique protein structures representative of the many protein conformations sampled during the simulation.

2.2. Initial AutoGrow runs

AutoGrow was run three times, once using a neuraminidase crystal structure (PDB ID: 2HU4, Russell et al., 2006) as the template protein and twice using each of the top two ensemble structures (Cheng et al., 2008). In each of these three runs, AutoGrow ran for eight generations, adding fragments to a core scaffold similar to oseltamivir. Each generation initially contained fifty ligands. For each generation after the first, 10 primary individuals were taken from the previous generation, based on both the score of the most populated docking cluster and successful active-site binding. An additional 20 “crossovers” and 20 “mutants” were created from these 10 primary individuals, subject to the requirement that all compounds contain fewer than 100 atoms. The first generation initially contained only the scaffold and 49 “mutants,” as no previous generation existed from which “parents” could be drawn for crossover production.

To determine fitness, all AutoGrow-generated ligands were docked into their respective neuraminidase structures (the crystal structure or the two ensemble conformations) using AutoDock 4.0.1 (Morris et al., 1998), a docking program with a physics-based scoring function that performs well relative to the scoring functions of other similar programs (e.g. DOCK, Flex, and GOLD, Rarey et al., 1996; Jones et al., 1997; Ewing et al., 2001; Bursulaya et al., 2003). Docking parameters were optimized for the positive-control docking of oseltamivir into the group-1 neuraminidase (N1) crystal structure. The initial AutoDock population size was set to 200 individuals, the maximum number of energy evaluations to 7×10^6 , the number of runs to 25, and the RMSD tolerance to 2.0. All other AutoDock parameters were set to the default values. The AutoDock-predicted binding energy was taken to be the energy associated with the most populated AutoDock cluster. AutoDock grids were calculated for regularly spaced points at intervals of 0.375 Å contained within a cube $24.00 \text{ Å} \times 27.00 \text{ Å} \times 24.75 \text{ Å}$, centered on the neuraminidase active site.

2.3. A novel fragment library derived from FDA-approved compounds

To generate novel compounds, AutoGrow drew upon a new fragment library containing 37 637 redundant fragments derived from FDA-approved compounds using an in-house script called *Fragmentizer*. To create this novel fragment library, we first obtained the names of hundreds of FDA-approved compounds by searching Drugs@FDA, supplemented with a list provided by the laboratory of Maurizio Pellecchia. The PDB structures of these compounds were downloaded from drugbank.ca (Wishart et al., 2006) and filtered to remove those with molecular weight greater than 700 g/mol. After additional processing, 1174 drugs remained.

For each compound, *Fragmentizer* first identified all single bonds that could be broken without altering the electronic or geometric configuration of neighboring atoms. The program next generated a second list of all possible bond combinations. Each compound was then decomposed by simultaneously cutting all the bonds of each combination and adding hydrogen atoms to the resulting fragments as needed. Following compound decomposition, all fragments with mass greater than 150 Da were removed, leaving 37 637 fragments. Redundant fragments were not eliminated. Both *Fragmentizer* and the novel fragment library

derived from FDA-approved compounds can be downloaded from http://www.nbcr.net/software/downloads/virtual_lib/.

2.4. Post-processing of AutoGrow-generated compounds

As a beta version of AutoGrow was used to generate the ligands, the compounds had to be further processed to correct occasional structural errors. The top 10 ligands from each of the three AutoGrow runs were visually inspected. Where the atoms of two distinct fragments were very close, those fragments were bound together to form rings. Where two fragments were mistakenly added via the same scaffold linker hydrogen, extra atoms were removed as needed. Additionally, some sulfur atoms were bound to too many hydrogen atoms. These were eliminated or replaced with oxygen atoms as necessary. Following corrections, each ligand underwent 500 steps of Cartesian minimization in ICM (Molsoft), a molecular modeling and docking program, prior to being evaluated for drug likeness (Table 1 and Table S1).

2.5. Relaxed complex docking

The relaxed complex scheme (Amaro et al., 2008a) was used to rescore predicted inhibitors. All compounds were docked into the 27 ensemble configurations using AutoDock 4.0.1 (Morris et al., 1998). Additionally, six positive controls were included: sialic acid, the natural neuraminidase substrate, in the boat, chair, and twist conformations; zanamivir and oseltamivir, FDA-approved neuraminidase inhibitors; and peramivir, a compound currently in clinical trials. An ensemble-average AutoDock score was calculated for each ligand by averaging the AutoDock scores and weighting according to the cluster population size (Table 1 and Table S1):

$$\bar{E} = \frac{\sum_{i=1}^{23} w_i E_i}{\sum_{i=1}^{23} w_i} \quad (1)$$

where \bar{E} is the weighted ensemble-average score, w_i is the size of cluster i , and E_i is the AutoDock score of the ligand docked into the centroid of cluster i .

The docking parameters were unchanged, except that the maximum number of energy evaluations was decreased to 5×10^6 , and the number of runs was increased to 100.

2.6. Compound modification

The top predicted ligand from each of the three AutoGrow runs (compounds 1, 2, and 3; Table 1 and Table S1), as judged by the ensemble-average score, was selected for further examination. Each of these three ligands was loaded into ICM (Molsoft), together with the corresponding ensemble member that gave the best score, and redocked using the ICM docking program (Molsoft). This initial docking established a baseline score that was subsequently used to judge whether modifications to the compound improved or reduced binding affinity.

Each of the three ligands then underwent a series of manual modifications, producing 14 novel drug-like compounds. Modifications were made such that the ICM docking score was maintained, drug-like metrics (molecular weight, number of hydrogen-bond acceptors and donors, predicted $\text{Log}P$, etc.) were improved, chirality was reduced, and molecular rigidity was increased. Furthermore, visual inspection led to the addition of some novel groups that AutoGrow had not suggested. These “modified compounds” were rescored using the relaxed complex scheme, with the same AutoDock and AutoGrid parameters used previously.

Table 1

The initial AutoGrow-generated compounds prior to modification, ranked according to the ensemble-average AutoDock score. The six positive controls are also included.

| | Ensemble-average AutoDock score | Molecular Weight | HBA | HBD | Log <i>P</i> |
|---|---------------------------------|------------------|-----|-----|--------------|
| 1 | -12.83 | 503.24 | 12 | 10 | -2.89 |
| 2 | -11.13 | 337.19 | 6 | 5 | -1.71 |
| 3 | -11.06 | 335.18 | 6 | 4 | -1.75 |
| | -8.24 | 284.17 | 4 | 4 | 2.03 |
| | | | | | |
| | -7.67 | | | | |
| | -7.39 | | | | |

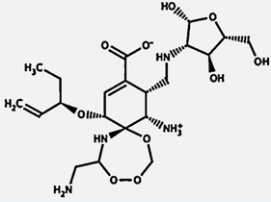
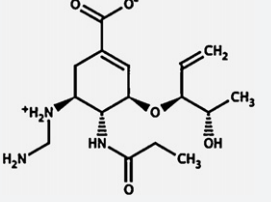
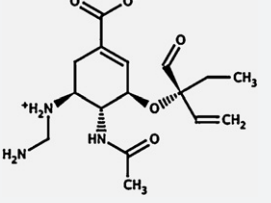
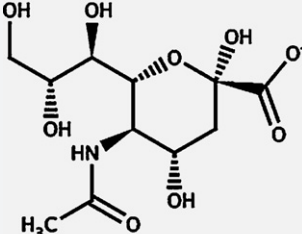
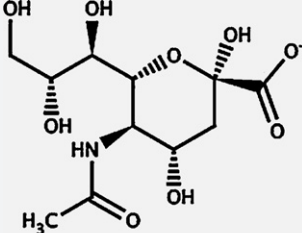
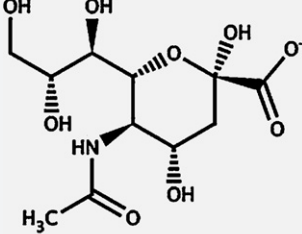
| | | | | | |
|---|--|--|--|--|--|
|  | | | | | |
| (Oseltamivir) | | | | | |
|  | | | | | |
| (Peramivir) | | | | | |
|  | | | | | |
| (Zanamivir) | | | | | |

Table 1 (Continued)

| | Ensemble-average AutoDock score | Molecular Weight | HBA | HBD | Log P |
|---|---------------------------------|------------------|-----|-----|-------|
|  (SIA Boat) | -6.20 | | | | |
|  (SIA Twist) | -5.89 | | | | |
|  (SIA Chair) | -4.94 | | | | |

3. Results and discussion

The influenza virus has caused several pandemics in the last century; recently, a new pandemic strain (H1N1) has been identified (Dawood et al., 2009). In preparation for pandemic influenza, many nations have stockpiled inhibitors of the influenza protein neuraminidase (Oxford et al., 2004). Unfortunately, drug-resistant strains have emerged (Kiso et al., 2004; Beigel et al., 2005; de Jong et al., 2005; De Clercq, 2006), and the need for novel neuraminidase inhibitors is great.

Neuraminidase has highly flexible loops adjacent to its sialic acid binding site. In the first crystal structures of group-1 neuraminidase (N1), the so-called 150-loop adopted an open conformation not seen in previous crystal structures of group-2 proteins (N2) (Russell et al., 2006). Under different crystallographic conditions, however, the N1 150-loop adopted a closed conformation similar to that of N2 (Varghese et al., 1983; Baker et al., 1987). The flexibility of this loop in N1, as well as implications for drug design, have been further characterized via molecular dynamics simulations (Amaro et al., 2007; Cheng et al., 2008).

The great flexibility of the N1 active site defies traditional computer-aided drug-design efforts, which typically focus on static crystal structures and at best account for only limited protein flexibility. To aid future drug-design efforts, Cheng et al. recently performed a 40-ns molecular dynamics simulation of the N1 holo enzyme (Cheng et al., 2008). 1.6×10^4 protein conformations were extracted at regular intervals and clustered into 27

groups using root-mean-square-deviation (RMSD) conformational clustering. The set of the corresponding 27 distinct centroids, representative of all conformations sampled, is said to constitute an *ensemble*.

3.1. Initial compound generation

In some fragment-based drug-design strategies, weakly binding molecular fragments, identified experimentally via X-ray crystallography or NMR, or computationally via computer docking, are linked to generate potent composite inhibitors (Rees et al., 2004). An alternate computational fragment-based growing strategy, exemplified by programs like LUDI (Bohm, 1992, 1993, 1994) and AutoGrow (Durrant et al., 2009), adds small molecular fragments to initial scaffolds known to bind the target protein, with the goal of improving binding affinity. Because fragment-based strategies are combinatorial, a far greater diversity of compounds can be synthesized and tested than would be possible with traditional high-throughput assays.

To generate predicted ligands, we used a beta version of the computer program AutoGrow (Durrant et al., 2009), an evolutionary algorithm that automates fragment addition to core scaffolds. Each member of a population of AutoGrow-generated compounds was evaluated for binding using AutoDock; the best predicted binders became the founding members of the next generation, wherein fragments were again added/modified. Generation after generation, ligands eventually evolved that were well suited to the

Table 2

The most common fragments from the library derived by decomposing FDA-approved drugs.

| Rank | Compound | Percent of library |
|------|--|--------------------|
| 1 | CH ₄ | 11.71% |
| 2 | H ₃ C-CH ₃ | 4.79% |
| 3 | H ₂ O | 4.28% |
| 4 | CH ₃ -CH ₂ -CH ₃ | 2.49% |
| 5 | H ₃ C-OH | 1.93% |
| 6 | H ₃ C-NH ₂ | 1.64% |
| 7 | H ₂ C=O | 1.40% |
| 8 | CH ₃ -CH ₂ -OH | 1.31% |
| 9 | CH ₃ -NH-CH ₂ -CH ₃ | 1.29% |
| 10 | benzene | 1.28% |

template protein structures specified. AutoGrow was initially run against an N1 crystal structure (PDB ID: 2HU4) (Russell et al., 2006). To account for neuraminidase flexibility, the program was run twice more against the top two representative ensemble conformations.

AutoGrow drew upon a fragment library derived from FDA-approved compounds. The library was generated by decomposing approved drugs into their constituent fragments using an in-house script. As AutoGrow selects fragments from the library at random, redundant fragments were maintained to bias the program towards those fragments most commonly found in FDA-approved drugs. For example, the most common fragment (methane) constituted 11.71% of the library. The 10 most abundant fragments of this new library are listed in Table 2. Thirty compounds, 10 from each AutoDock run, were considered candidates for further analysis.

3.2. Relaxed complex rescoring

To further account for N1 flexibility, these compounds were reranked using the relaxed complex scheme (Amaro et al., 2008a). In a traditional virtual screen, a docking program is used to predict the ligand energy of binding to a static structure, usually obtained from X-ray crystallography or NMR. The relaxed complex scheme builds upon this traditional methodology by docking candidate ligands into multiple protein conformations extracted from a molecular dynamics simulation. Compounds are then ranked by the ensemble-average predicted binding energy, rather than by the score associated with a single static structure alone. The relaxed complex scheme has been used to identify inhibitors of FKBP (Lin et al., 2002), HIV integrase (Schames et al., 2004), and *Trypanosoma brucei* RNA editing ligase 1 (Amaro et al., 2008b).

In addition to rescoring the 30 AutoGrow-generated compounds, we also scored six positive controls: sialic acid, the natural neuraminidase substrate, in the boat, chair, and twist conformations; zanamivir and oseltamivir, FDA-approved neuraminidase inhibitors; and peramivir, a compound currently in clinical trials (Table 1 and Table S1). The measured IC₅₀ values of oseltamivir, peramivir, and zanamivir are 0.33 ± 0.27, 0.37 ± 0.26, and 0.57 ± 0.46 nM, respectively (Malaisree et al., 2008). These IC₅₀ values are roughly three orders of magnitude smaller than the ensemble-average AutoDock-predicted inhibition constants of 2.25, 5.01, and 8.58 μM, respectively. However, there is a clear correlation between prediction and measurement ($R^2 = 0.92$), and, importantly, the relaxed complex scheme ranked the known neuraminidase inhibitors correctly.

The experimentally measured K_i of sialic acid suggests that binding to the natural substrate is much weaker. The measured K_i of 50 μM (Colman, 1994) corresponds well with the ensemble-average AutoDock-predicted inhibition constants of 33.67, 68.02, and 375.48 μM for sialic acid in the boat, twist, and chair conformation, respectively. When the lowest predicted sialic-acid inhibition

constant is considered, the overall correlation between prediction and measurement is further strengthened ($R^2 = 0.97$).

This strong correlation demonstrates that, while the ensemble-average predicted binding energies and inhibition constants are not numerically accurate, the relaxed complex scheme can be used to accurately rank candidate neuraminidase inhibitors. Notably, all 30 AutoGrow-generated compounds ranked better than currently approved neuraminidase inhibitors when the relaxed complex scheme was used; the score of the best novel compound was −12.83 kcal/mol, compared to −8.24 kcal/mol for the best FDA-approved inhibitor, oseltamivir.

3.3. Compound modification

Despite the use of fragments derived from FDA-approved drugs, the AutoGrow-generated compounds were not particularly drug like. Consequently, the top ligand from each of the three AutoGrow runs (compounds 1, 2, and 3; Table 1 and Table S1), as judged by the ensemble-average score, was selected for further examination. Fourteen drug-like compounds were subsequently generated by making manual modifications to the three lead ligands. Manual modifications were guided by six rules: satisfy Lipinski's rule of five (Lipinski et al., 2001), conserve the predicted binding affinity, remove buried unpaired hydrogen-bond donors and acceptors, increase molecular rigidity, and reduce chirality.

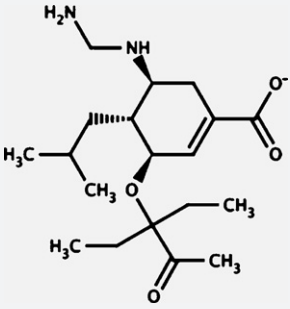
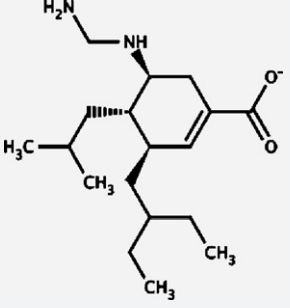
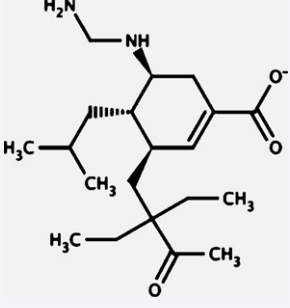
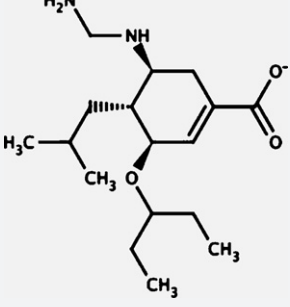
Lipinski's rule of five. The AutoDock-generated compounds were generally too large, leading to multiple Lipinski violations (Lipinski et al., 2001). Lipinski's rule of five, developed in 2001, states that compounds generally have poor absorption or permeation if they possess two or more of the following properties: more than 5 hydrogen-bond donors, more than 10 hydrogen-bond acceptors, a molecular weight greater than 500 Da, or a ClogP greater than five. As the AutoGrow-generated compounds were generally large, most contained too many hydrogen-bond donors and acceptors and too large a molecular weight. Manual modifications reduced the size of the candidate ligands so they would better conform to Lipinski's rule of five.

Predicted binding energy. The reduction in size was generally accompanied by a mild drop in the predicted binding affinity. Some interacting groups had to be removed in order to reduce the molecular weight. Additionally, most steps (i.e. chemical modifications) away from the AutoGrow-generated ligands, which had been "optimized" for binding energy, naturally reduced binding affinity. Nevertheless, the compounds were redocked with each manual modification, and modifications that caused precipitous drops in the predicted binding energy were rejected.

Hydrogen bonds. Some of the docked AutoGrow-generated compounds had hydrogen-bond donors and acceptors that were buried but unpaired (i.e. "unsatisfied"). The hydrogen-bond donors and acceptors of a fully hydrated ligand are typically satisfied via interactions with the water solvent. A large energy penalty occurs upon binding if unsatisfied hydrogen-bond donors and acceptors are positioned in solvent-inaccessible regions along the protein–ligand interface because a hydrogen bond with the water solvent is lost without the compensatory creation of a protein–ligand hydrogen bond. Some of the manual modifications made served to remove these unpaired hydrogen-bond donors and acceptors.

Compound rigidity. Additional manual modifications were made to increase compound rigidity. In the unbound state, non-rigid, "floppy" compounds undergo many different conformational transitions as they twist about their rotatable bonds. Upon binding, however, the ligand is stabilized, resulting in a large entropic penalty of binding. For rigid compounds, the difference in entropy between the bound and unbound state is not as great, and so the penalty is less.

Table 3
The top four modified compounds, as judged by the ensemble-average AutoDock score.

| | | Ensemble-average AutoDock score | Molecular Weight | HBA | HBD | Log P |
|---|---|---------------------------------|------------------|-----|-----|-------|
| 4 |  | -11.05 | 353.24 | 6 | 3 | 2.72 |
| 5 |  | -10.96 | 309.25 | 4 | 3 | 4.65 |
| 6 |  | -10.72 | 351.26 | 5 | 3 | 4.02 |
| 7 |  | -10.68 | 311.23 | 5 | 3 | 3.09 |

These modified compounds were rescored using the relaxed complex scheme (Table 3 and Table S2). Ten of the 14 modified compounds ranked better than FDA-approved neuraminidase inhibitors; the ensemble-average score of the best modified compound was -11.05 kcal/mol, compared to -8.24 kcal/mol for oseltamivir.

3.4. Analysis of the top four modified compounds

The top four modified compounds are all similar, in part because they are built on the same cyclohex-1-enecarboxylate scaffold. While similar to oseltamivir, the novel compounds are decorated with different molecular fragments that, in theory, serve to enhance the binding affinity.

All four compounds have a carboxylate group in the one position, similar to the known neuraminidase inhibitors oseltamivir, paramivir, and zanamivir. An examination of an oseltamivir-neuraminidase crystal structure (Russell et al., 2006) reveals that this carboxylate group participates in hydrogen bonds with R371 and Y347 (distance cutoff, 3.0 Å; angle cutoff, 30°). In addition, an analysis of the top four modified compounds docked into the 27 ensemble conformations suggests that the carboxylate group also forms hydrogen bonds with R292 and, on rare occasions, with R118 (Fig. 1).

All four modified compounds have an (aminomethyl)amino (aminal) group at the five position instead of an amino group, as in oseltamivir. The crystal structure demonstrates that the oseltamivir amine forms hydrogen bonds with D151 and E119. In contrast, an

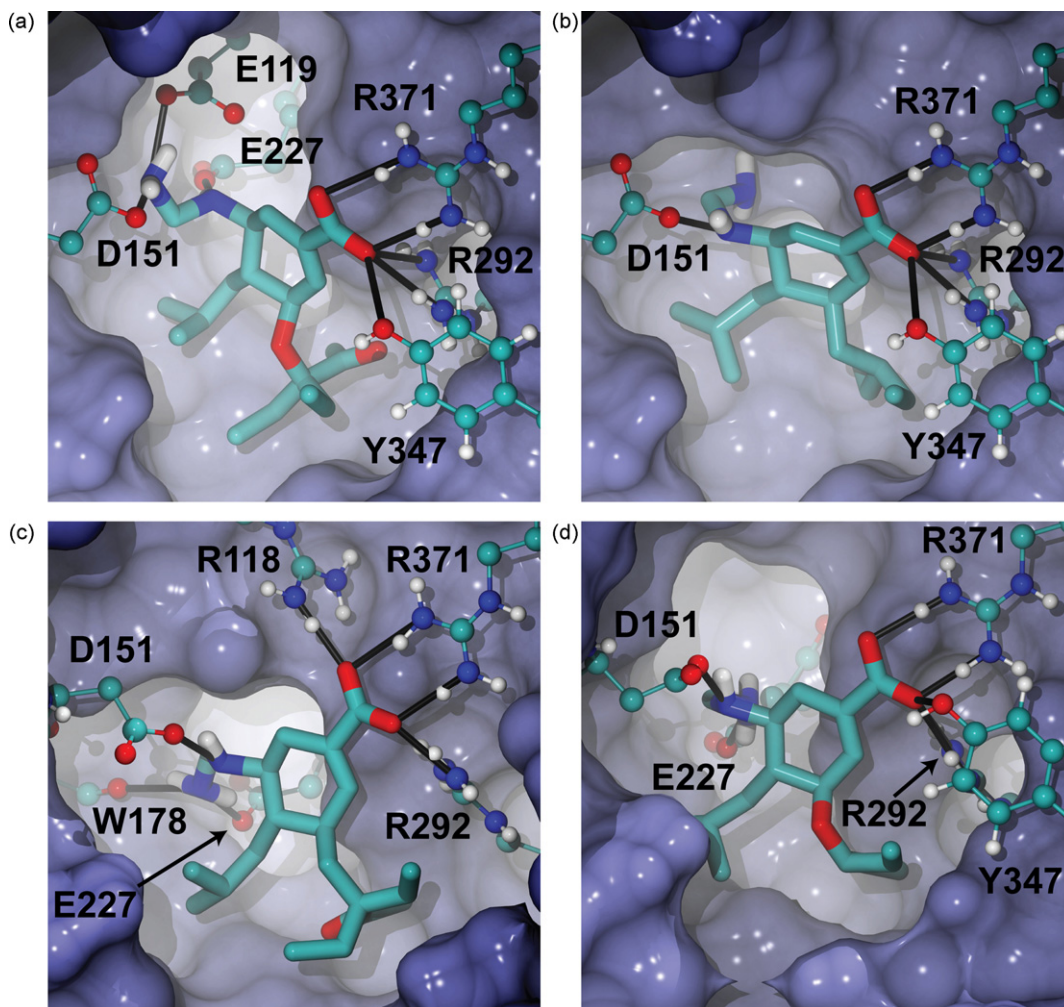


Fig. 1. The top four modified compounds docked into the ensemble conformation that gave the best predicted binding energy. Hydrogen bonds are shown as black lines. Some portions of the protein have been removed to facilitate visualization. (A) Compound 4. (B) Compound 5. (C) Compound 6. (D) Compound 7.

analysis of the top four modified compounds suggests that binding between the aminal fragment and residues D151 and E119 occurs only occasionally. Rather, the distal amine binds instead with E227 and, less frequently, with E277 and the backbone carbonyl of W178. In the case of compounds 5 and 7, the proximal amine is predicted to bind occasionally with E227 as well. Crystal structures indicate that the analogous guanidine groups of peramivir (Zhang et al., 1992) and zanamivir (Xu et al., 2008) likewise form hydrogen bonds with the backbone carbonyl of W178 (Fig. 1).

Unfortunately, aminal groups are unstable and subject to hydrolysis. Initial efforts to find alternative groups failed; for example, when the aminal was changed to a urea, the ensemble-average predicted binding energy was significantly reduced (data not shown). Another solution may be to replace the aminal with a guanidino group, which is essentially a rigid aminal with an additional amine bound to the bridging carbon atom. We again note that zanamivir and peramivir, neuraminidase inhibitors with IC_{50} 's comparable to that of oseltamivir (Malaisree et al., 2008), have guanidino groups at the analogous location. Alternatively, the proximal aminal nitrogen atom could be replaced with a carbon atom, though such a change may make synthesis more challenging.

The top four modified compounds contain a 2-methylpropyl group at the four position instead of the acetamido group characteristic of oseltamivir, peramivir, and zanamivir. The crystal structures of oseltamivir, peramivir, and zanamivir bound to neuraminidase

(Russell et al., 2006; Xu et al., 2008) suggest that a hydrogen bond may form between the acetamido carbonyl oxygen atom and R152, though in the case of oseltamivir the hydrogen bond is strained (D-H-A angle of 54°) (Russell et al., 2006). Additionally, the acetamido methyl group may contribute to the overall binding affinity via hydrophobic interactions with W178. We note, however, that the acetamido amine hydrogen, a hydrogen-bond donor, is buried and unpaired. Like the acetamido group, the 2-methylpropyl group of the top four modified compounds is likewise predicted to form hydrophobic interactions with W178, but without the need for a buried but unpaired hydrogen-bond donor (Fig. 1). We note, however, that, in addition to facilitating a hydrogen bond between the carbonyl oxygen atom and the receptor, the amide linker may also simplify chemical synthesis, and so may be necessary on those grounds.

Compounds 4, 5, and 6 have (3-ethyl-2-oxopentan-3-yl)oxy; 2-ethylbutyl; and 2,2-diethyl-3-oxobutyl groups, respectively, at the three position, instead of the pentan-3-yloxy group of oseltamivir. An analysis of the binding poses of the top four modified compounds suggests that the bridging oxygen atom of the oseltamivir pentan-3-yloxy fragment does not contribute significantly to the energy of binding. The crystal structure of oseltamivir bound to neuraminidase reveals no hydrogen bonds with this oxygen atom (Russell et al., 2006); additionally, an ensemble-wide analysis of compounds 4 and 7, which include the bridging oxygen atom, likewise revealed no hydrogen-bond formation (Fig. 1).

The importance of the bridging oxygen atom can be further assessed by comparing the predicted binding energies of compounds that differ only at this location. For example, the ensemble-average predicted binding energies of compounds 5 and 7 (Table 3), which differ only in the presence or absence of the bridging oxygen atom, are nearly identical. A comparison between compounds 4 and 6 gives a similar result (Table 3). Though the bridging oxygen is likely energetically unnecessary, we again note that it may greatly facilitate chemical synthesis.

The top four compounds all mimic oseltamivir at the three position in that they contain multiple aliphatic chains. However, compounds 4 and 6 also contain a carbonyl group, a potential hydrogen-bond acceptor. An analysis of these compounds docked into the 27 ensemble conformations revealed that the carbonyl oxygen atom is predicted to form occasional hydrogen bonds with R152. Additionally, the carbonyl oxygen atom of compound 4 forms occasional hydrogen bonds with R292, and the carbonyl oxygen atom of compound 6 forms occasional hydrogen bonds with N294 (Fig. 1).

4. Conclusion

Pandemic influenza (H1N1) poses an imminent threat, and drug-resistant strains have already emerged (Kiso et al., 2004; Beigel et al., 2005; de Jong et al., 2005; De Clercq, 2006). In the current work, the computer program AutoGrow (Durrant et al., 2009) was used to generate novel predicted neuraminidase inhibitors. Given the great flexibility of the N1 active site, protein dynamics were also incorporated into the computer-aided drug-design process. Several potential inhibitors were identified that are predicted to bind to neuraminidase better than current FDA-approved drugs.

The neuraminidase inhibitors oseltamivir and zanamivir, both FDA approved, have similar binding poses (Russell et al., 2006; Xu et al., 2008). Despite these similarities, these two compounds have very different resistance profiles. As of 2005, no virus resistant to zanamivir had been isolated from an immunocompetent patient, but resistance to oseltamivir was then emergent (Moscona, 2005). The principal difference between oseltamivir and zanamivir, and the difference likely responsible for their disparate resistance profiles, is the set of molecular fragments used to decorate the central six-member ring. We are therefore hopeful that the novel inhibitors suggested here, with their unique decorating fragments, may likewise serve as scaffolds for future neuraminidase inhibitors against which resistance has not yet developed.

Acknowledgements

JDD is funded by a Pharmacology Training Grant through the UCSD School of Medicine. This work was carried out with funding from NIH GM31749, NSF MCB-0506593, and MCA93S013 to JAM. Additional support from the Howard Hughes Medical Institute, the National Center for Supercomputing Applications, the San Diego Supercomputer Center, the W.M. Keck Foundation, Accelrys, Inc., the National Biomedical Computational Resource, and the Center for Theoretical Biological Physics is gratefully acknowledged. We would also like to thank Dr. Rommie E. Amaro for helpful discussions and support.

Appendix A. Supplementary data

Supplementary data associated with this article can be found, in the online version, at doi:10.1016/j.compbiolchem.2010.03.005.

References

- Abdel-Ghaffar, A.N., Chotpitayasonondh, T., Gao, Z., Hayden, F.G., Nguyen, D.H., de Jong, M.D., Naghdaliyev, A., Peiris, J.S., Shindo, N., Soeroro, S., Uyeki, T.M., 2008. Update on avian influenza A (H5N1) virus infection in humans. *N. Engl. J. Med.* 358, 261–273.
- Amaro, R.E., Baron, R., McCammon, J.A., 2008a. An improved relaxed complex scheme for receptor flexibility in computer-aided drug design. *J. Comput.-Aided Mol. Des.* 22, 693–705.
- Amaro, R.E., Schnauffer, A., Interthal, H., Hol, W., Stuart, K.D., McCammon, J.A., 2008b. Discovery of drug-like inhibitors of an essential RNA-editing ligase in *Trypanosoma brucei*. *Proc. Natl. Acad. Sci.* 105, 17278–17283.
- Amaro, R.E., Minh, D.D., Cheng, L.S., Lindstrom Jr., W.M., Olson, A.J., Lin, J.H., Li, W.W., McCammon, J.A., 2007. Remarkable loop flexibility in avian influenza N1 and its implications for antiviral drug design. *J. Am. Chem. Soc.* 129, 7764–7765.
- Baker, A.T., Varghese, J.N., Laver, W.G., Air, G.M., Colman, P.M., 1987. Three-dimensional structure of neuraminidase of subtype N9 from an avian influenza virus. *Proteins* 2, 111–117.
- Beigel, J.H., Farrar, J., Han, A.M., Hayden, F.G., Hyer, R., de Jong, M.D., Lochindarat, S., Nguyen, T.K., Nguyen, T.H., Tran, T.H., Nicoll, A., Touch, S., Yuen, K.Y., 2005. Avian influenza A (H5N1) infection in humans. *N. Engl. J. Med.* 353, 1374–1385.
- Bohm, H.-J., 1992. The computer program LUDI: a new method for the de novo design of enzyme inhibitors. *J. Comput.-Aided Mol. Des.* 6, 61.
- Bohm, H.J., 1993. A novel computational tool for automated structure-based drug design. *J. Mol. Recogn.* 6, 131.
- Bohm, H.J., 1994. On the use of LUDI to search the Fine Chemicals Directory for ligands of proteins of known three-dimensional structure. *J. Comput.-Aided Mol. Des.* 8, 623–632.
- Bursulaya, B.D., Totrov, M., Abagyan, R., Brooks III, C.L., 2003. Comparative study of several algorithms for flexible ligand docking. *J. Comput. Aided Mol. Des.* 17, 755–763.
- Cheng, L.S., Amaro, R.E., Xu, D., Li, W.W., Arzberger, P.W., McCammon, J.A., 2008. Ensemble-based virtual screening reveals potential novel antiviral compounds for avian influenza neuraminidase. *J. Med. Chem.* 51, 3878–3894.
- Christen, M., Hunenberger, P.H., Bakowies, D., Baron, R., Burgi, R., Geerke, D.P., Heinz, T.N., Kastenholz, M.A., Krautler, V., Oostenbrink, C., Peter, C., Trzesniak, D., van Gunsteren, W.F., 2005. The GROMOS software for biomolecular simulation: GROMOS05. *J. Comput. Chem.* 26, 1719–1751.
- Colman, P.M., 1994. Influenza virus neuraminidase: structure, antibodies, and inhibitors. *Protein Sci.* 3, 1687–1696.
- Daura, X., Gademann, K., Jaun, B., Seebach, D., van Gunsteren, W.F., Mark, A.E., 1999. Peptide folding: when simulation meets experiment. *Angew. Chem. Int. Ed.* 38, 236–240.
- Dawood, F.S., Jain, S., Finelli, L., Shaw, M.W., Lindstrom, S., Garten, R.J., Gubareva, L.V., Xu, X., Bridges, C.B., Uyeki, T.M., 2009. Emergence of a novel swine-origin influenza A (H1N1) virus in humans. *N. Engl. J. Med.* 360, 2605–2615.
- De Clercq, E., 2006. Antiviral agents active against influenza A viruses. *Nat. Rev. Drug Discov.* 5, 1015–1025.
- De Clercq, E., Neyts, J., 2007. Avian influenza A (H5N1) infection: targets and strategies for chemotherapeutic intervention. *Trends Pharmacol. Sci.* 28, 280–285.
- de Jong, M.D., Tran, T.T., Truong, H.K., Vo, M.H., Smith, G.J., Nguyen, V.C., Bach, V.C., Phan, T.Q., Do, Q.H., Guan, Y., Peiris, J.S., Tran, T.H., Farrar, J., 2005. Oseltamivir resistance during treatment of influenza A (H5N1) infection. *N. Engl. J. Med.* 353, 2667–2672.
- Durrant, J.D., Amaro, R.E., McCammon, J.A., 2009. AutoGrow: a novel algorithm for protein inhibitor design. *Chem. Biol. Drug Des.* 73, 168–178.
- Ewing, T.J., Makino, S., Skillman, A.G., Kuntz, I.D., 2001. DOCK 4.0: search strategies for automated molecular docking of flexible molecule databases. *J. Comput.-Aided Mol. Des.* 15, 411.
- Jones, G., Willett, P., Glen, R.C., Leach, A.R., Taylor, R., 1997. Development and validation of a genetic algorithm for flexible docking. *J. Mol. Biol.* 267, 727.
- Kiso, M., Mitamura, K., Sakai-Tagawa, Y., Shiraiishi, K., Kawakami, C., Kimura, K., Hayden, F.G., Sugaya, N., Kawaoka, Y., 2004. Resistant influenza A viruses in children treated with oseltamivir: descriptive study. *The Lancet* 364, 759–765.
- Kobasa, D., Kodihalli, S., Luo, M., Castrucci, M.R., Donatelli, L., Suzuki, Y., Suzuki, T., Kawaoka, Y., 1999. Amino acid residues contributing to the substrate specificity of the influenza A virus neuraminidase. *J. Virol.* 73, 6743–6751.
- Lin, J.H., Perryman, A.L., Schames, J.R., McCammon, J.A., 2002. Computational drug design accommodating receptor flexibility: the relaxed complex scheme. *J. Am. Chem. Soc.* 124, 5632–5633.
- Lipinski, C.A., Lombardo, F., Dominy, B.W., Feeney, P.J., 2001. Experimental and computational approaches to estimate solubility and permeability in drug discovery and development settings. *Adv. Drug Deliv. Rev.* 46, 3–26.
- Malaisree, M., Rungrotmongkol, T., Decha, P., Intharathep, P., Aruksakunwong, O., Hannongbua, S., 2008. Understanding of known drug–target interactions in the catalytic pocket of neuraminidase subtype N1. *Proteins* 71, 1908–1918.
- Morris, G.M., Goodsell, D.S., Halliday, R.S., Huey, R., Hart, W.E., Belew, R.K., Olson, A.J., 1998. Automated docking using a Lamarckian genetic algorithm and an empirical binding free energy function. *J. Comput. Chem.* 19, 1639–1662.
- Moscona, A., 2005. Oseltamivir resistance—disabling our influenza defenses. *N. Engl. J. Med.* 353, 2633–2636.
- Oxford, J., Balasingam, S., Lambkin, R., 2004. A new millennium conundrum: how to use a powerful class of influenza anti-neuraminidase drugs (NAIs) in the community. *J. Antimicrob. Chemother.* 53, 133–136.
- Rarey, M., Kramer, B., Lengauer, T., Klebe, G., 1996. A fast flexible docking method using an incremental construction algorithm. *J. Mol. Biol.* 261, 470.

- Rees, D.C., Congreve, M., Murray, C.W., Carr, R., 2004. Fragment-based lead discovery. *Nat. Rev. Drug Discov.* 3, 660–672.
- Russell, R.J., Haire, L.F., Stevens, D.J., Collins, P.J., Lin, Y.P., Blackburn, G.M., Hay, A.J., Gamblin, S.J., Skehel, J.J., 2006. The structure of H5N1 avian influenza neuraminidase suggests new opportunities for drug design. *Nature* 443, 45–49.
- Schames, J.R., Henchman, R.H., Siegel, J.S., Sotriffer, C.A., Ni, H., McCammon, J.A., 2004. Discovery of a novel binding trench in HIV integrase. *J. Med. Chem.* 47, 1879–1881.
- Varghese, J.N., Laver, W.G., Colman, P.M., 1983. Structure of the influenza virus glycoprotein antigen neuraminidase at 2.9 Å resolution. *Nature* 303, 35–40.
- Wishart, D.S., Knox, C., Guo, A.C., Shrivastava, S., Hassanali, M., Stothard, P., Chang, Z., Woolsey, J., 2006. DrugBank: a comprehensive resource for in silico drug discovery and exploration. *Nucleic Acids Res.* 34, D668–D672.
- Xu, X., Zhu, X., Dwek, R.A., Stevens, J., Wilson, I.A., 2008. Structural characterization of the 1918 influenza virus H1N1 neuraminidase. *J. Virol.* 82, 10493–10501.
- Zhang, X.J., Baase, W.A., Matthews, B.W., 1992. Multiple alanine replacements within alpha-helix 126–134 of T4 lysozyme have independent, additive effects on both structure and stability. *Protein Sci.* 1, 761–776.